Long-period surface structure stabilized by Fermi surface nesting: Cu(001)-(root 20x root 20)R26.6 degrees-In

AUTHOR(S):

Nakagawa, T; Yeom, HW; Rotenberg, E; Krenzer, B; Kevan, SD; Okuyama, H; Nishijima, M; Aruga, T

CITATION:

Nakagawa, T ...[et al]. Long-period surface structure stabilized by Fermi surface nesting: Cu(001)-(root 20x root 20)R26.6 degrees-In. PHYSICAL REVIEW B 2006, 73(7): 075407.

ISSUE DATE:

2006-02

URL:

http://hdl.handle.net/2433/50057

PHYSICAL REVIEW B **73**, 075407 (2006)

Long-period surface structure stabilized by Fermi surface nesting: Cu(001)-($\sqrt{20}\times\sqrt{20}$)R26.6°-In

T. Nakagawa,[1,*] H. W. Yeom,[2] E. Rotenberg,[3] B. Krenzer,[4] S. D. Kevan,[4] H. Okuyama,[1] M. Nishijima,[1] and T. Aruga[1,†]
[1]*Department of Chemistry, Graduate School of Science, Kyoto University, Kyoto 606-8502, Japan*
[2]*Center for Atomic Wires and Layers and Institute of Physics and Applied Physics, Yonsei University, Seoul 120-749, Korea*
[3]*Advanced Light Source (ALS), Ernest Orlando Lawrence, Berkeley National Laboratory, Berkeley, California 94720, USA*
[4]*Department of Physics, University of Oregon, Eugene, Oregon 97403, USA*
(Received 1 November 2005; revised manuscript received 15 December 2005; published 2 February 2006)

We have studied the atomic and electronic structure of the Cu(001)-($\sqrt{20}\times\sqrt{20}$)R26.6°-In surface, which undergoes a reversible transition to a $p(2\times2)$ phase at high temperature. Low temperature scanning-tunneling microscopy indicates a $p(2\times2)$ structure modulated at the ($\sqrt{20}\times\sqrt{20}$) periodicity. Angle-resolved photoelectron spectroscopy shows a surface resonance exhibiting gap opening and backfolding along a ($\sqrt{20}\times\sqrt{20}$) zone boundary. We suggest that the ($\sqrt{20}\times\sqrt{20}$) structure is stabilized due to the Fermi surface nesting accompanying a surface charge density wave.

DOI: 10.1103/PhysRevB.73.075407 PACS number(s): 73.20.At, 68.35.Bs, 71.45.Lr

I. INTRODUCTION

Bulk elemental metals usually have structures with high spatial symmetries such as hexagonal closed packed, face- and body-centered cubic. This is also the case for monolayers of elemental metals on flat surfaces, which tend to have two-dimensional high symmetry structures. For monolayers of alkali metals, other than Li, on flat metal surfaces, hexagonal or quasihexagonal structures are usually observed,[1] the latter being understood as due to the competition of isotropic adatom-adatom cohesive interaction with the periodic potential exerted by the substrate. However, monolayers of heavier p-block metals (In, Tl, Pb, Bi) often exhibit complex structures with periods of several nanometers.[2]

While the electronic origin for the long periodicity is usually unrevealed, the angle-resolved photoelectron spectroscopy (ARPES) work on Cu(001)-($9\sqrt{2}\times2\sqrt{2}$)R45°-In showed that the strong electron-phonon coupling associated with the partial Fermi-surface nesting is responsible for this long-period structure.[3] The work showed that the ($9\sqrt{2}\times2\sqrt{2}$)R45°-In surface undergoes a phase transition at ~350 K to a high-temperature (HT) $p(2\times2)$ phase. The phase transition was accompanied with the disappearance of the energy gap at the Fermi level. This indicates that the long-period, low-temperature phase is the ground state stabilized by low electronic energy but is destabilized at high temperatures with respect to a short-period "metallic" phase by the electronic entropy term of the free energy. This is analogous to the charge-density-wave (CDW) phase observed in quasi-2D bulk materials such as the $\sqrt{13}\times\sqrt{13}$ structure in TaS_2.[4]

In this work, the atomic and electronic structure of the ($\sqrt{20}\times\sqrt{20}$)R26.6° (referred to below by $\sqrt{20}$) phase on In/Cu(001) has been studied. As shown in the previous work,[5] three ordered structures are formed below a monolayer coverage upon In deposition on Cu(001) at room temperature. The $\sqrt{20}$ has the highest In coverage among them. Scanning-tunneling microscopy (STM) indicates that the $\sqrt{20}$ surface is composed of an approximate $p(2\times2)$ unit but is modulated strongly at the $\sqrt{20}$ periodicity. The electronic energy band shows the coexistence of backfolded and metallic bands over a circular-shaped Fermi surface (FS), indicating partial FS nesting. We propose that the $\sqrt{20}$ structure is sta-

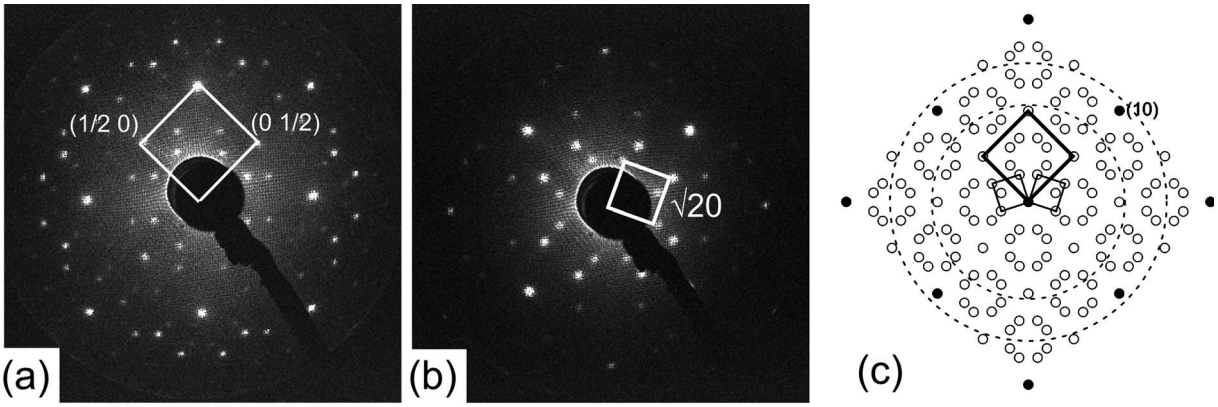

FIG. 1. LEED pattern for the ($\sqrt{20}\times\sqrt{20}$)R26.6°-In surface at the primary energy of (a) 90 eV, and (b) 60 eV. (c) Schematics of the LEED pattern. Solid and open circles represent diffraction spots due to (1×1) and $\sqrt{20}$ periodicities, respectively. Dotted circles represent the area observed in (a) and (b).

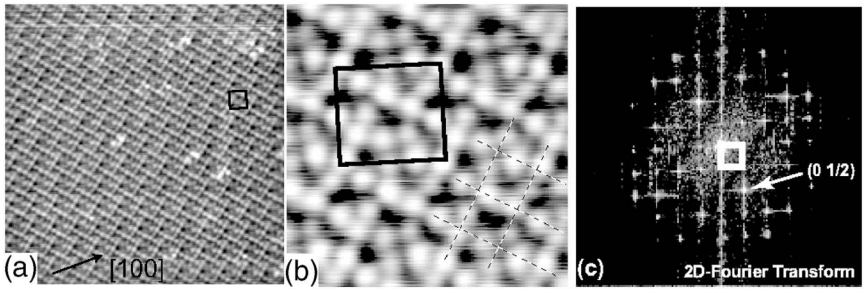

FIG. 2. (a) STM image for the $(\sqrt{20}\times\sqrt{20})R26.6°$ phase (V_s =−7 mV, I_t=1 nA, 150×150 Å^2), and (b) zoomed-up image (V_s=−7 mV, I_t=10 nA, 30×30 Å^2). The solid and broken lines represent unit cells of $(\sqrt{20}\times\sqrt{20})R26.6°$ and $p(2\times2)$, respectively. (c) Fourier transform of the STM image shown in (a).

bilized by the Fermi surface nesting at a high-order surface Brillouin zone (SBZ) boundary near the FS.

II. EXPERIMENT

A commercial variable-temperature STM was used in a constant current mode. The ARPES experiment was performed at the 7.0.3 beamline of Advanced Light Source, Berkeley, with a photon energy of 80 eV and energy and angular resolutions of 50 meV and 0.1°, respectively. In was deposited with the sample kept at 300 K. The In coverage is given below in units of ML, which is defined as 1 ML=1.53 $\times10^{19}$ m^{-2}, the atom density of the Cu(001) surface. All the measurements were done on the as-grown sample. For experimental details, see the previous publication.[6]

III. RESULTS

In Fig. 1 we show the low energy electron diffraction (LEED) patterns taken at 110 K, which exhibit strong integer and half order spots and numerous clear but weak satellite spots, suggesting that the long range order develops well. The satellite spots are explained by $\sqrt{20}$ diffraction.

With increasing sample temperature the satellite spots become weak quickly at ~450 K, while the half order ones do not show such a change, suggesting that the surface undergoes a phase transition from the $\sqrt{20}$ to $p(2\times2)$ phase. While the $\sqrt{20}$ pattern revives after quick cooling down from above the transition temperature, prolonged annealing above 450 K results in a $c(4\times4)$ LEED pattern after cooling down. The $c(4\times4)$ phase has a lower In coverage,[5] which suggests that the desorption or penetration of In atoms takes place above ~450 K. Thus we were not able to make a detailed study of the HT phase.

Figure 2(a) shows an STM image for a flat $\sqrt{20}$ terrace. The corrugation amplitude of the $\sqrt{20}$ structure is about 0.3 Å. The image also shows a few bright protrusions with a height of 1.5–2.0 Å, which we attribute to excess In atoms. Note that the excess In atoms do not affect the $\sqrt{20}$ structure

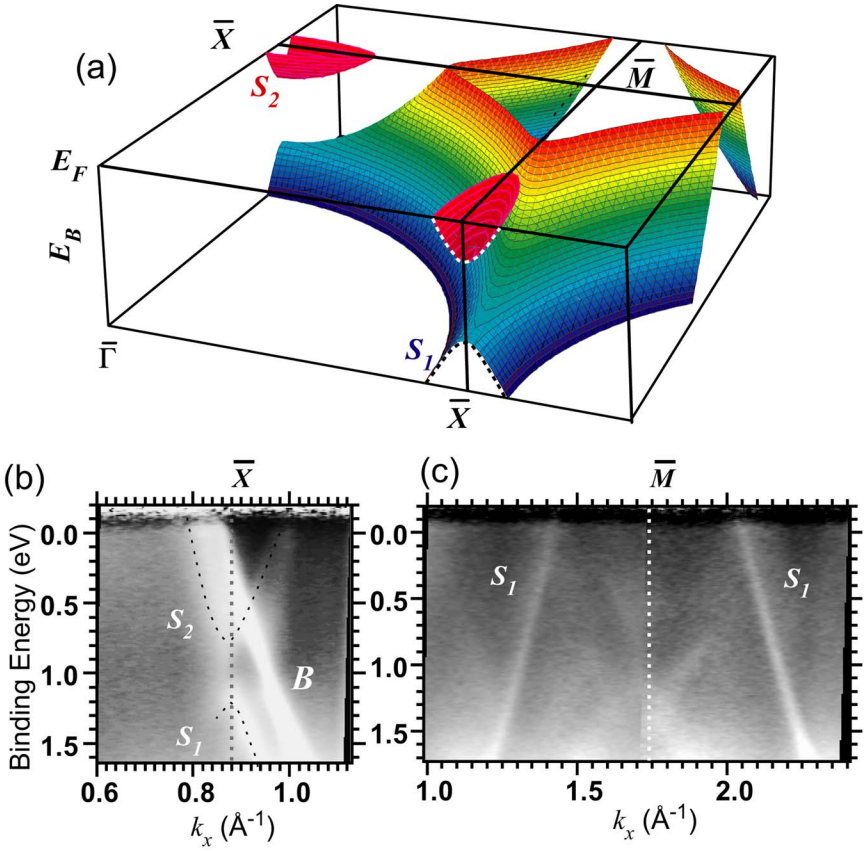

FIG. 3. (Color online) (a) Schematic drawing of the In-induced surface resonance bands on Cu(001). S_1 and S_2 denote surface resonance bands originating from In-Cu interface. (b) Electronic band map along $\bar{\Gamma}$-$\bar{X}$. B denotes the bulk Cu 4sp band. (b) Electronic band map along $\bar{\Gamma}$-$\bar{M}$. The photoemission intensity is normalized to the Fermi distribution function.

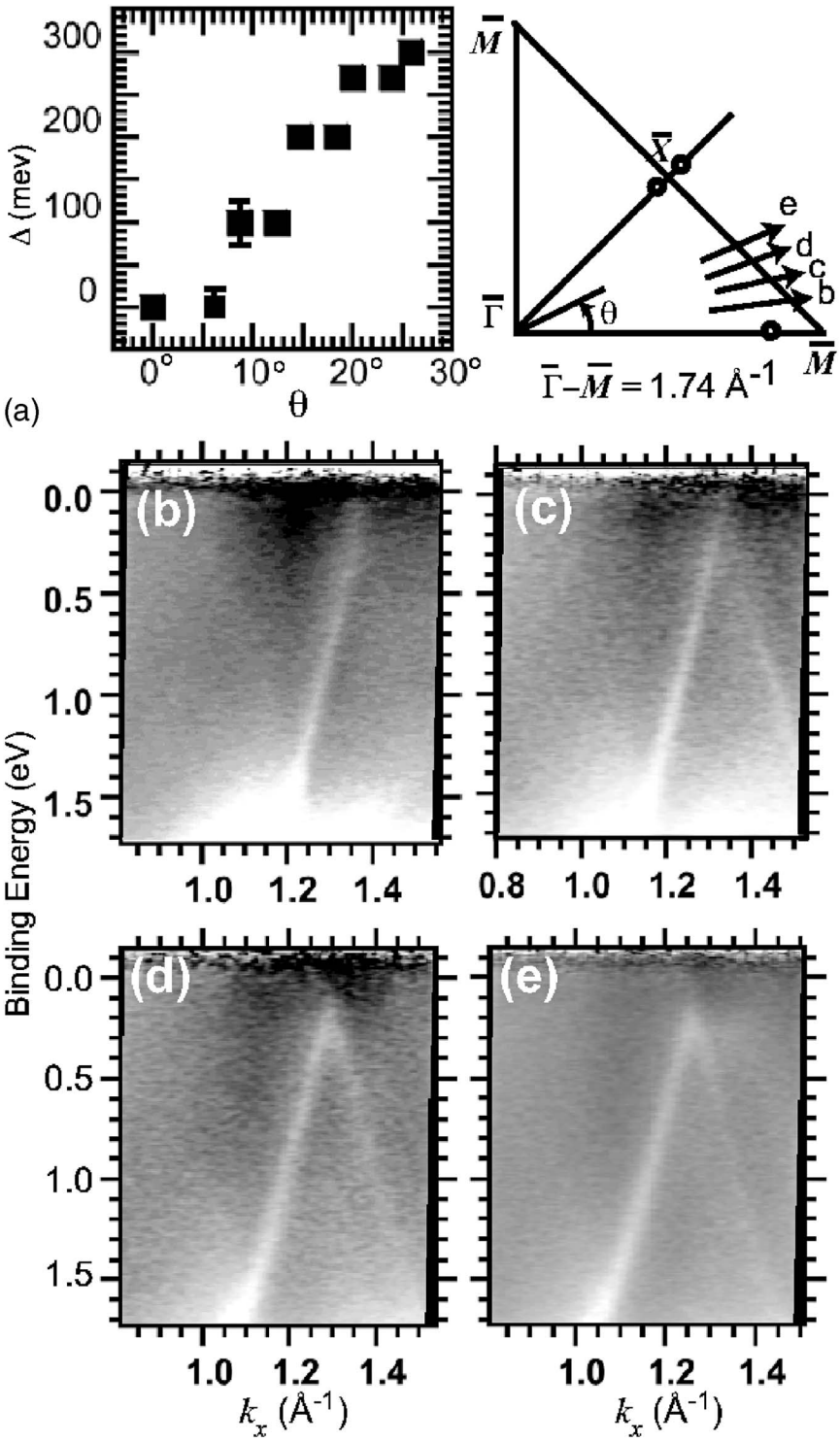

FIG. 4. (a) The minimum binding energy of the S_1 band as a function of the angle from the [100] azimuth. The arrows (b)–(e) in the right panel indicate the paths along which the band maps shown in (b)–(e) are measured. The circles indicate the Fermi wave vectors along $\bar{\Gamma}$-$\bar{M}$ and $\bar{\Gamma}$-$\bar{X}$. (b)–(e) Electronic band maps taken at azimuthal angles indicated in (a) as a function of the momentum components along $\bar{\Gamma}$-$\bar{M}$, k_x. The photoemission intensity is normalized to the Fermi distribution function.

around them. Figure 2(b) shows a high resolution STM image of the $\sqrt{20}$ surface. All the protrusions lie approximately on the $p(2\times2)$ mesh indicated by broken lines but are not in exact agreement with the $p(2\times2)$ symmetry. The unit cell corresponds to $\sqrt{20}$. The Fourier transform of the STM image is shown in Fig. 2(c), which shows a $\sqrt{20}$ reciprocal lattice with strong intensity at (0 1/2) position. This is in good agreement with the LEED result. (Note that the reciprocal lattice points only from a single domain are found in the Fourier transform of the STM image.)

The $\sqrt{20}$-In surface has a nearly-free-electron-like circular Fermi surface constituted by In-induced interface resonance bands. Figure 3(a) shows a schematic band structure of In-induced surface resonance bands for non-CDW phases.[5,7] Figure 3(b) shows an ARPES band map taken along $\bar{\Gamma}$-$\bar{X}$. Three bands, labeled S_1, S_2, and B, are observed. The B band is present also on the clean Cu(001) surface and its position is dependent on photon energy, which indicates that the B band is due to the bulk Cu-4sp band. The S_1 and S_2 bands are induced by In adsorption. The S_1 band is backfolded at $\bar{X}$

with the minimum binding energy of 1.1 eV. The S_2 band, which was not clearly visible in the previous work[5] using He-I radiation, is also backfolded at $\bar{X}$ but to the direction opposite to S_1. At $\bar{X}$ the S_1 and S_2 bands are separated from each other by ~0.2 eV. The existence of the hybridization gap at the surface Brillouin zone (SBZ) boundary of 1×1 indicates that the two surface bands have the same symmetry.

In Fig. 3(c) the electronic band structure along $\bar{\Gamma}$-$\bar{M}$ is shown. Only the S_1 band is observed, which crosses E_F at 1.44 Å^{-1} in the first (1×1) SBZ and at 2.04 Å^{-1} in the second. The SBZ boundary, $\bar{M}$, is located at 1.74 Å^{-1}, which suggests that the second band is formed due to the substrate (1×1) potential. Besides, several weak bands can be recognized, which may be assigned to replicas due to the $\sqrt{20}$ periodic potential. We, however, could not clearly observe the replicas associated with the $\sqrt{20}$ symmetry, which may be due to weak surface lattice contribution to photoemission structure factor.

In Figs. 4(b)–4(e) we show band maps for the S_1 band taken along the azimuthal angles increasingly rotated from the [100] direction. The S_1 band is metallic along $\bar{\Gamma}$-$\bar{M}$ as shown in Fig. 3(c). Upon going away from the [100] azimuth, the S_1 band is backfolded below E_F and exhibits a band gap [Figs. 4(c)–4(e)]. The magnitude of the energy gap increases upon going away from the [100] azimuth. In Fig. 4(a), we show the minimum binding energy of the S_1 band at the backfolding point as a function of the angle θ from the [100] azimuth. The energy gap monotonically increases with increasing θ from 0° to 30°. For $\theta>30°$, the band gap quickly diminishes and the S_2 band comes down below E_F as shown in Fig. 3(b).

IV. DISCUSSION

Twelve protrusions per unit cell are observed in the STM image [Fig. 2(b)], which corresponds to 0.6 ML if we assign each protrusion to a single In atom. This coverage is lower than that for the $c(4\times4)$ surface. The $\sqrt{20}$ phase appears above $\theta_{In}=0.8$ ML as studied by Auger electron spectroscopy (AES) and LEED.[5] Thus STM does not image all the In atoms. It is speculated that a $p(2\times2)$ alloy layer is formed below the topmost $\sqrt{20}$ layer. If this is the case, not only the surface $\sqrt{20}$ structure but also a $p(2\times2)$ structure contribute to the $p(2\times2)$ diffraction spots. In this case the In coverage should be $0.60+0.25n$ [n is the number of subsurface In atoms per $p(2\times2)$ unit cell]. Considering the AES and LEED results, the ideal coverage for the $\sqrt{20}$ phase is estimated to be 0.85, which is in agreement with the previous result.[7]

The formation of energy gaps should be associated with the lattice potential with corresponding k vector. In Fig. 5, the k points where the S_1 band is backfolded is shown by triangles, which shows that the "ridge" of the S_1 band is aligned on a straight line (gap line). If this straight line perpendicularly bisects the line joining $\bar{\Gamma}_{00}$ and any reciprocal lattice point, then the backfolding, or the gap formation, should be related with the lattice potential associated with the wave vector represented by that reciprocal lattice point.

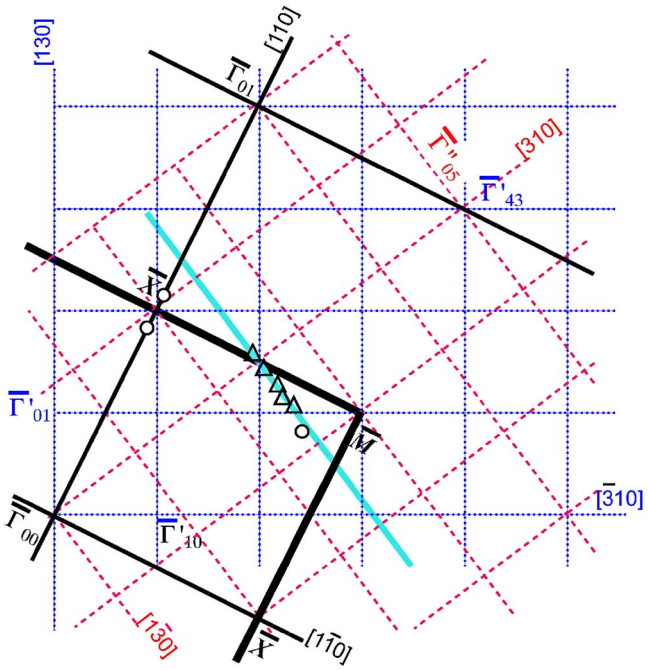

FIG. 5. (Color online) The k points where the S_1 band is backfolded (triangles) and reciprocal lattices: thick and thin solid (black) lines indicate SBZ and reciprocal lattice, respectively, of (1×1); dotted (blue) and dashed (red) lines indicate reciprocal lattices for two equiprobable $\sqrt{20}$ structures rotated by 53.1° from each other. The reciprocal lattice points are indicated by $\bar{\Gamma}_{nm}$ for (1×1) and $\bar{\Gamma}'_{n'm'}$ and $\bar{\Gamma}''_{n''m''}$ for two $\sqrt{20}$ structures, where n, m, n', m', n'', and m'' denote integers. Circles indicate the k positions where the S_1 and S_2 bands cross E_F. A gray (blue) solid line indicates SBZ boundary created by Γ'_{43} and Γ''_{05}.

The gap line does not bisect the line joining $\bar{\Gamma}_{00}$ and any reciprocal lattice points for (1×1), which suggests that the gap formation is not due to the (1×1) lattice potential. In Fig. 5, we also show the reciprocal lattices for the $\sqrt{20}$ structure, in two equiprobable orientations, by dotted and dashed lines. The gap line bisects perpendicularly the line joining $\bar{\Gamma}_{00}$ and $\bar{\Gamma}'_{43}$, a reciprocal lattice point in one of the two $\sqrt{20}$ domains, which coincides $\bar{\Gamma}''_{05}$ in the other domain. In other words, the gap line coincides one of the Brillouin zone boundaries ($Q=1.37$ Å^{-1}) of the $\sqrt{20}$ structure. This suggests that the band gap is formed by the lattice potential of $\sqrt{20}$.

Thus we conclude that the $\sqrt{20}$ periodicity on this surface is stabilized by the Peierls-type CDW formation mechanism as in the other phases on In/Cu(001) (Refs. 3 and 6) and Sn/Cu(001).[8]

The detection of the new periodicity generated by the FS nesting is often difficult. This may be because the intensity of the backfolded band, which is proportional to the strength of electron-phonon coupling and the new lattice potential,[9,10] is rather weak in many CDW systems.[10,11] On other surface CDW phases, $(9\sqrt{2}\times2\sqrt{2})R45°$ and $c(4\times4)$, on In/Cu(001) and a similar one on Sn/Cu(001), the band gaps are rather large (~1 eV) and the backfolded band is clearly observed. This indicates that the CDW phase transitions on these sur-

faces are driven by a mechanism[12,13] similar to that for the strong-coupling CDW transition.[4,14,15] However, as already pointed out,[12,13] the CDW transition mechanism on metal surfaces differs from those in bulk materials. While the energetic stability of the CDW ground state is governed by overall surface band gap, defined by the energy difference between the lower band maximum and the upper band minimum, the electronic entropy is dominated by the energy difference between E_F and the upper band minimum. This causes the duality of the surface CDW transitions.[6] On the other hand, the energy gap (energy difference between E_F and the lower band maximum) on the $\sqrt{20}$ surface is relatively small (~300 meV). This implies that the electron-phonon coupling or the lattice modulation of $\sqrt{20}$ is weak. While we do not know the energy position of the upper band on this surface, the $\sqrt{20}$ phase may be closer to the weak-coupling regime than the phases mentioned above.

In summary, we have studied atomic and electronic structures of the Cu(001)-$(\sqrt{20}\times\sqrt{20})R26.6°$-In surface. The $(\sqrt{20}\times\sqrt{20})R26.6°$ surface undergoes a phase transition at ~450 K to $p(2\times2)$ upon heating. The STM shows In atoms arranged according to $(\sqrt{20}\times\sqrt{20})R26.6°$ symmetry. All the atoms are approximately located on the $p(2\times2)$ mesh, which is in accordance with the strong $p(2\times2)$ diffraction intensity in the LEED. ARPES for $(\sqrt{20}\times\sqrt{20})R26.6°$ shows energy gap at E_F along the SBZ boundary. The $(\sqrt{20}\times\sqrt{20})R26.6°$-In structure is stabilized by the energy gain associated with the Fermi surface nesting.

ACKNOWLEDGMENT

H.W.Y. was supported by KOSEF through CAWL at Yonsei University of the CRi program.

*Present address: Institute for Molecular Science, Okazaki 444-8585, Japan.
†Electronic address: aruga@kuchem.kyoto-u.ac.jp

[1] T. Aruga and Y. Murata, Prog. Surf. Sci. **31**, 61 (1989).
[2] T. Aruga, J. Phys.: Condens. Matter **14**, 8393 (2002).
[3] T. Nakagawa, G. I. Boishin, H. Fujioka, H. W. Yeom, I. Matsuda, N. Takagi, M. Nishijima, and T. Aruga, Phys. Rev. Lett. **86**, 854 (2001).
[4] G. Grüner, *Density Waves in Solids* (Addison-Wesley, Reading, MA, 1994).
[5] T. Nakagawa, S. Mitsushima, H. Okuyama, M. Nishijima, and T. Aruga, Phys. Rev. B **66**, 085402 (2002).
[6] T. Nakagawa, H. Okuyama, M. Nishijima, T. Aruga, H. W. Yeom, E. Rotenberg, B. Krenzer, and S. D. Kevan, Phys. Rev. B **67**, 241401(R) (2003).
[7] S. Hatta, H. Okuyama, M. Nishijima, and T. Aruga, Appl. Surf. Sci. **237**, 270 (2004).
[8] J. Martínez-Blanco, V. Joco, H. Ascolani, A. Tejeda, C. Quirós, G. Panaccione, T. Balasubramanian, P. Segovia, and E. G. Michel, Phys. Rev. B **72**, 041401(R) (2005).
[9] J. Voit, L. Perfetti, F. Zwick, H. Berger, G. Margaritondo, G. Grüner, H. Hochst, and M. Grioni, Science **290**, 501 (2000).
[10] V. Brouet, W. L. Yang, X. J. Zhou, Z. Hussain, N. Ru, K. Y. Shin, I. R. Fisher, and Z. X. Shen, Phys. Rev. Lett. **93**, 126405 (2004).
[11] Th. Straub, Th. Finteis, R. Claessen, P. Steiner, S. Hüfner, P. Blaha, C. S. Oglesby, and E. Bucher, Phys. Rev. Lett. **82**, 4504 (1998).
[12] S. Hatta, H. Okuyama, M. Nishijima, and T. Aruga, Phys. Rev. B **71**, 041401(R) (2005).
[13] S. Hatta, H. Okuyama, T. Aruga, and O. Sakata, Phys. Rev. B **72**, 081406(R) (2005).
[14] W. L. McMillan, Phys. Rev. B **16**, 643 (1977).
[15] E. Tosatti, in *Electronic Surface States and Interface States on Metallic Systems*, edited by E. Bertel and D. Donath (World Scientific, Singapore, 1995), p. 67.